ISSN 0016-2663, *Functional Analysis and Its Applications*, 2024, *Vol.* 58, *No.* 2, *pp.* 143–159.

Russian Text ©*The Author(s)*, 2024, *published in Funktsional'nyi Analiz i Ego Prilozheniya*, 2024, *Vol.* 58, *No.* 2, *pp.* 52–71.

Elliptic Analogue of the Vershik–Kerov Limit Shape

Andrei Grekov and Nikita Nekrasov

Dedicated to the 90*th anniversary of Anatoly Moiseevich Vershik, with admiration*

Abstract. We review the limit shape problem for the Plancherel measure and its generalizations found in supersymmetric gauge theory instanton count. We focus on the measure, interpolating between the Plancherel measure and the uniform measure, a $U(1)$ case of $\mathcal{N} = 2^*$ gauge theory. We give the formula for its limit shape in terms of elliptic functions, generalizing the trigonometric "arcsin" law of Vershik–Kerov and Logan–Schepp.

Key words: limit measures, limit shape, spectral curves, instantons, enumerative geometry.

DOI: 10.1134/S0016266324020059

1. Introduction

In their seminal paper [6], A. Vershik and S. Kerov studied the large N asymptotics of the Plancherel measure on the set of irreducible representations R_λ of symmetric group $S(N)$:

$$\mu[\lambda] = \frac{(\dim R_\lambda)^2}{N!}. \tag{1.1}$$

To R_λ one associates the Young diagram λ

$$\lambda = (\lambda_i), \qquad \lambda_1 \geqslant \lambda_2 \geqslant \cdots \geqslant \lambda_{\ell(\lambda)} > 0, \tag{1.2}$$

with

$$|\lambda| = N = \lambda_1 + \lambda_2 + \cdots + \lambda_{\ell(\lambda)} \tag{1.3}$$

boxes. The main result of [6] is that upon rescaling the linear size of λ by $\sqrt{N}$, one finds, in the $N \to \infty$ limit, a piecewise smooth curve $f(x)$ (*the arcsin law*), which is read off a certain rational curve Σ through a solution of the Riemann-Hilbert problem. This limit shape curve determines the large N asymptotics of expectation values of all the moments (cf. [15]):

$$\mathbf{p}_k[\lambda] = (1 - 2^{-k})\zeta(-k) + \sum_{i=1}^{\infty}\left(\lambda_i - i + \frac{1}{2}\right)^k - \left(-i + \frac{1}{2}\right)^k. \tag{1.4}$$

Random Young diagrams behave in a similar way to large N random $N \times N$ matrices.

In this small note, we will study a one-parametric family of random partition models, motivated by the studies of supersymmetric gauge theories in four dimensions [11]. The measure (1.1) arises in a limit. To be more precise, the original Vershik–Kerov problem can be equivalently studied in the macrocanonical ensemble, where one sums over all N with the weight $\frac{1}{N!}z^N$. The parameter z is called fugacity. Instead of the large N limit, one studies the large z limit. It is this ensemble that we generalize below.

The paper is organized as follows. In section § 2, we rederive the main result of [6] using the language of qq-characters [14], [13]. In section § 3, we introduce our generalization of the macrocanonical ensemble, the corresponding qq-character. In section § 4, we solve the limit shape problem by using factorization of the *theta-transform* of the qq-character. In section § 5, we discuss various limits of our solution: comparison with the Vershik–Kerov limit shape, as well as the edge behavior. In section § 6, we discuss future directions, including the *higher times* generalizations of the problem.

2020 *Mathematics Subject Classification*: 60F15, 14H81, 81Q60.

2. Profiles, Limit Shapes, the Arcsin Law

We will use the results and notation from [11].

The Plancherel measure (1.1) is a probablity measure on the set of Young diagrams of fixed size N where

$$\sum_{\lambda,\,|\lambda|=N} \mu[\lambda] = 1. \tag{2.1}$$

In the studies of four-dimensional gauge theory [12], one arrives at a similar measure, but defined on the set of all Young diagrams with the size $N = |\lambda|$ weighted with a fugacity factor

$$\boldsymbol{\mu}_{\Lambda,\hbar}(\lambda) = \frac{1}{Z}\frac{1}{N!}\left(\frac{\mathrm{i}\Lambda}{\hbar}\right)^{2N}\mu[\lambda], \tag{2.2}$$

where the parameters Λ and $\hbar$ have the meaning of the instanton counting parameter and the $SU(2)$-rotation equivariant parameter, respectively. The normalization factor Z is given by

$$Z = \sum_{\lambda}\left(\frac{\mathrm{i}\Lambda}{\hbar}\right)^{2|\lambda|}\prod_{\square\in\lambda}\frac{1}{h_{\square}^2}, \tag{2.3}$$

where $h_{\square}$ - is the hook length of a box (i,j) in the Young diagram λ

$$h_{i,j} = \lambda_i - j + \lambda_j^t - i + 1. \tag{2.4}$$

Let x be an indeterminate. Define the $\mathbf{Y}(x)$-observable on the set of all Young diagrams by

$$\mathbf{Y}(x)|_{\lambda} = x\prod_{\square\in\lambda}\frac{(x-\hbar c_{\square})^2-\hbar^2}{(x-\hbar c_{\square})^2}, \tag{2.5}$$

where for $\square = (i,j) \in \lambda$, its *content* is defined by

$$c_{i,j} = i - j. \tag{2.6}$$

By cancellation of factors in the product, it could be also written as

$$\mathbf{Y}(x)|_{\lambda} = x\prod_{i=1}^{\ell_\lambda}\frac{x-\hbar i}{x+\hbar(\lambda_i-i)}\,\frac{x+\hbar(\lambda_i-i+1)}{x+\hbar(1-i)} = \frac{\prod_{\square\in\partial_+\lambda}(x-\hbar c_{\square})}{\prod_{\blacksquare\in\partial_-\lambda}(x-\hbar c_{\blacksquare})}, \tag{2.7}$$

where $\lambda_i = 0$ for $i > \ell_\lambda = \lambda_1^t$, and $\partial_+\lambda$ and $\partial_-\lambda$ are the sets of boxes which can be added to or removed from λ, respectively.

Obviously, the expectation value

$$\langle\mathbf{Y}(x)\rangle := \sum_{\lambda}\mu_{\Lambda,\hbar}[\lambda]\mathbf{Y}(x)|_{\lambda} \tag{2.8}$$

has poles as a function of x. Define another observable, the *character*, as

$$\boldsymbol{\chi}(x)|_{\lambda} = \mathbf{Y}(x)|_{\lambda} + \frac{\Lambda^2}{\mathbf{Y}(x)|_{\lambda}}. \tag{2.9}$$

It was proven in [13] that the expectation value $\langle\boldsymbol{\chi}(x)\rangle$ of the qq-character is pole-free. From (2.5), (2.9) we see that

$$\mathbf{Y}(x), \boldsymbol{\chi}(x) \sim x + O\left(\frac{1}{x^2}\right) \quad \text{as} \quad x\to\infty, \tag{2.10}$$

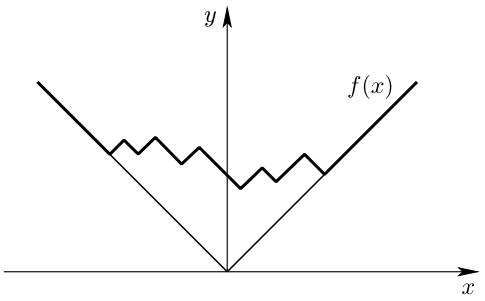

Fig. 1. Young diagram profile function.

and hence

$$\langle \boldsymbol{\chi}(x) \rangle = x. \tag{2.11}$$

Now we are ready to apply the main result of [11]. Namely, in the limit $\hbar \to 0$, the correlation functions defined using the measure (2.2) factorize

$$\langle \mathcal{O}_1 \mathcal{O}_2 \rangle = \langle \mathcal{O}_1 \rangle \langle \mathcal{O}_2 \rangle + o(\hbar), \qquad \hbar \to 0. \tag{2.12}$$

Thus, they become evaluations on the limit shape λ^∞, defined as a C^0 limit $f(x)$ (in fact, the limit is in C^1) of the profile function $f_\lambda(x)$ (cf. [11]):

$$\begin{aligned} f_\lambda(x) := |x| + \sum_{i=1}^{\infty} \big(& |x - \hbar(\lambda_i - i + 1)| \\ & - |x - \hbar(\lambda_i - i)| + |x + \hbar i| - |x + \hbar(i-1)| \big). \end{aligned} \tag{2.13}$$

We give an example of the profile $f_\lambda(x)$ below (Fig. 1). The $\mathbf{Y}(x)$-observable is expressed through the profile function via [11]

$$\mathbf{Y}(x)|_\lambda = \exp\left\{ \frac{1}{2} \int_{\mathbb{R}} \log(x-y) f_\lambda''(y)\, dy \right\}. \tag{2.14}$$

This follows from formula (2.7) by direct calculation. The factorization (2.12) is proven using the standard argument [6] as follows. The measure (2.2) scales as

$$\begin{aligned} \boldsymbol{\mu}_{\Lambda,\hbar}(\lambda) &= (1 + O(\hbar)) \\ &\quad \times \exp\left\{ \frac{1}{2\hbar^2} \text{v.p.} \int_{\mathbb{R}^2} dx_1\, dx_2 f_\lambda''(x_1) f_\lambda''(x_2) (x_1 - x_2)^2 \left(\log\left(\frac{x_1 - x_2}{\Lambda} \right) - \frac{3}{2} \right) \right\}, \end{aligned} \tag{2.15}$$

while the entropy factor, the number of configurations λ whose profile is C^0-close to $f(x)$, grows as

$$\propto \exp\left\{ c \frac{L_\lambda}{\hbar} \right\}, \tag{2.16}$$

where L_λ is a length of the boundary of λ measured in $\hbar$-units, $L = \hbar(\lambda_1^t + \lambda_1)$, and c is a constant of order 1. Thus, in the $\hbar \to 0$ limit,

$$\langle \mathbf{Y}(x) \rangle \to Y(x), \qquad \langle \mathbf{Y}(x)^{-1} \rangle \to \frac{1}{Y(x)}, \tag{2.17}$$

with

$$Y(x) = \exp\left\{ \frac{1}{2} \int_{\mathbb{R}} \log(x-y) f''(y)\, dy \right\}, \tag{2.18}$$

so that (2.11) becomes the equation of the rational curve

$$x = Y(x) + \frac{\Lambda^2}{Y(x)}. \tag{2.19}$$

Taking the derivative of (2.18), one gets

$$G(x) := \frac{d}{dx}\log Y(x) = \frac{1}{2}\int_{\mathbb{R}} \frac{f''(y)}{x-y}\,dy, \tag{2.20}$$

a function admitting analytic continuation to the complex plane $x \in \mathbb{C}$, with a branch cut on the support of $f''(x)$. The jump of $G(x)$ across the cut is equal to

$$G(x+\mathrm{i}0) - G(x-\mathrm{i}0) = \mathrm{i}\pi f''(x). \tag{2.21}$$

To read off $f''(x)$, we compare the expression above to the solution of (2.19):

$$Y(x) = \frac{x}{2} + \frac{1}{2}\sqrt{x^2 - 4\Lambda^2}. \tag{2.22}$$

Eq. (2.19) has two solutions for $Y(x)$ in terms of x. The "+" branch of the square root in (2.22) is chosen so as to give the correct large x asymptotics (2.10). Taking the derivative, we arrive at

$$G(x) = \frac{1}{\sqrt{x^2 - 4\Lambda^2}}. \tag{2.23}$$

It has a branch cut from -2Λ to 2Λ. Calculating the jump across it, we arrive at the expression for $f''(x)$ (for $|x| < 2\Lambda$)

$$f''(x) = \frac{1}{\pi\Lambda}\frac{1}{\sqrt{1-(x/(2\Lambda))^2}}. \tag{2.24}$$

The size of the corresponding partition asymptotes to

$$N \sim \frac{1}{4\hbar^2}\int_{\mathbb{R}} f''(x)x^2\,dx = \frac{\Lambda^2}{2\hbar^2}. \tag{2.25}$$

Integrating (2.24) once gives

$$f'(x) = \frac{2}{\pi}\arcsin\frac{x}{2\Lambda}, \tag{2.26}$$

and by integrating twice, we prove the following theorem.

Theorem (see [6] and [8]). *The limit shape of the distribution* (1.1) *on the set of Young diagrams of size* N *as* $\hbar \sim \Lambda/\sqrt{2N} \to 0$ *is described by the profile*

$$f_{\mathrm{VK}}(x) = \begin{cases} \dfrac{2}{\pi}\left(x\arcsin\dfrac{x}{2\Lambda} + \sqrt{4\Lambda^2 - x^2}\right), & |x| \leqslant 2\Lambda, \\ |x|, & |x| \geqslant 2\Lambda, \end{cases} \tag{2.27}$$

representing the $\hbar$*-rescaled piece-wise linear boundary of* λ.

Remark. Mathematicians usually present (2.27) with $\Lambda = 1$. Keeping Λ as a parameter is motivated by generalizations involving, e.g., several random Young diagrams [12].

3. Elliptic Generalization of the Vershik–Kerov Model

In this section, we are introducing a one parameter deformation of (2.2). It arises in the studies of mass-deformed maximally supersymmetric gauge theory, the so-called $\mathcal{N} = 2^*$ theory [12]:

$$\boldsymbol{\mu}_{m,\mathfrak{q},\hbar}[\lambda] = \frac{\mathfrak{q}^{|\lambda|}}{Z_{2^*}(m,\mathfrak{q},\hbar)} \prod_{\square\in\lambda} \left(1 - \left(\frac{m}{\hbar h_\square}\right)^2\right), \tag{3.1}$$

with the normalization partition function Z_{2^*} defined such that $\sum_\lambda \boldsymbol{\mu}_{m,\mathfrak{q},\hbar}[\lambda] = 1$[1]. The fugacity

$$\mathfrak{q} = e^{2\pi i\tau} \tag{3.2}$$

is usually written in terms of the modular parameter

$$\tau = \frac{\vartheta}{2\pi} + \frac{4\pi \mathrm{i}}{g^2} \tag{3.3}$$

of the elliptic curve underlying the microscopic $\mathcal{N} = 4$ theory [3], in agreement with the Montonen–Olive S-duality conjecture [16]. Mathematically, the measure makes sense for any complex values m and $\mathfrak{q}$ such that $|\mathfrak{q}| < 1$; however, in order for it to be a positive definite distribution on the set of all Young diagrams, we restrict $\mathfrak{q} \in \mathbb{R}$, and $m \in \mathrm{i}\mathbb{R}$.

The $\mathbf{Y}(x)$-observable is defined, as before, by (2.5), while the definition of the qq-character is much more involved (cf. Eq. (153) in the arxiv version of [13]; see also [14], where the $\hbar \to 0$ limit was analyzed):

$$\boldsymbol{\chi}(x) = \sum_\nu \boldsymbol{\mu}_{\hbar,\mathfrak{q},m}[\nu] \frac{\prod_{\square\in\partial_+\nu} \mathbf{Y}(x + mc_\square)}{\prod_{\square\in\partial_-\nu} \mathbf{Y}(x + mc_\square)}. \tag{3.4}$$

In (3.4) the sum is taken over the set of auxiliary Young diagrams ν, not to be confused with the diagrams λ of the original ensemble (3.1). Note that the roles of m and $\hbar$ in (3.4) are switched when compared to (3.1).

The main theorem of [13] implies that the expectation value

$$\langle \boldsymbol{\chi}(x) \rangle_{2^*} := \sum_\lambda \boldsymbol{\mu}_{m,\mathfrak{q},\hbar}[\lambda] \boldsymbol{\chi}(x)|_\lambda \tag{3.5}$$

has no poles in x, behaves as x for large x; therefore, it is equal to x

$$\langle \boldsymbol{\chi}(x) \rangle_{2^*} = x. \tag{3.6}$$

4. Solving for the Limit Shape in the Elliptic Case

In the limit $\hbar \to 0$, the same arguments as in § 3 show that the expectation values of $\mathbf{Y}(x)$ tend to evaluations on the limit shape $\lambda^\infty_{2^*}$:

$$\begin{aligned} \langle \mathbf{Y}(x) \rangle_{2^*} &\xrightarrow[\hbar\to 0]{} Y(x), \\ \langle \boldsymbol{\chi}(x) \rangle_{2^*} &\xrightarrow[\hbar\to 0]{} \phi(\mathfrak{q}) \sum_\nu \mathfrak{q}^{|\nu|} \frac{\prod_{\square\in\partial_+\nu} Y(x + mc_\square)}{\prod_{\square\in\partial_-\nu} Y(x + mc_\square)}, \end{aligned} \tag{4.1}$$

[1] In [11], [13] an explicit formula for Z_{2^*} can be found, but we don't need it here.

where

$$\phi(\mathfrak{q}) = \prod_{n=1}^{\infty}(1-\mathfrak{q}^n). \tag{4.2}$$

Comparing (4.1) and (3.6), we get the functional equation

$$\frac{x}{\phi(\mathfrak{q})} = \sum_{\nu} \mathfrak{q}^{|\nu|} \frac{\prod_{\square\in\partial_+\nu} Y(x+mc_\square)}{\prod_{\square\in\partial_-\nu} Y(x+mc_\square)} \tag{4.3}$$

for $Y(x)$, replacing Eq. (2.19) of the Vershik–Kerov problem. It would appear impossible to solve the infinite order non-linear difference equation Eq. (4.3). However, it is solvable by what we call the *θ-transform*. Fix $z \in \mathbb{C}^\times$– the spectral parameter in the world of integrable systems. Apply

$$\chi(x) \mapsto \sum_{n\in\mathbb{Z}} (-z)^n \mathfrak{q}^{(n^2-n)/2} \chi(x+mn) \quad \text{for} \quad z \in \mathbb{C}^* \tag{4.4}$$

to both sides of Eq. (4.3). Using the factorization formula proven in § 7, one arrives at

$$\begin{aligned} x\theta(z;\mathfrak{q}) + mz\frac{d}{dz}\theta(z;\mathfrak{q}) = \phi(\mathfrak{q})Y(x) \prod_{n=0}^{\infty}\left(1 - z\mathfrak{q}^n \frac{Y(x+(n+1)m)}{Y(x+nm)}\right) \\ \times \prod_{n=1}^{\infty}\left(1 - z^{-1}\mathfrak{q}^n \frac{Y(x-nm)}{Y(x-(n-1)m)}\right), \end{aligned} \tag{4.5}$$

where

$$\theta(z;\mathfrak{q}) := \sum_{n\in\mathbb{Z}} (-z)^n \mathfrak{q}^{(n^2-n)/2} = (1-z)\prod_{n=1}^{\infty}(1-\mathfrak{q}^n)(1-z\mathfrak{q}^n)(1-z^{-1}\mathfrak{q}^n). \tag{4.6}$$

By comparing the expressions for zeros of the LHS and the RHS of the equality above, we will be able to express $Y(x)$ in terms of x as explicitly as needed to find the limit shape profile. Indeed, from the LHS we see that its zeros are described by (cf. [11] where this was derived via another method)

$$x = x(z) = -mz\frac{d}{dz}\log\theta(z;\mathfrak{q}) = m\left(\frac{z}{1-z} + \sum_{n=1}^{\infty}\left(\frac{z\mathfrak{q}^n}{1-z\mathfrak{q}^n} + \frac{\mathfrak{q}^n}{\mathfrak{q}^n - z}\right)\right). \tag{4.7}$$

As a function of z, x obeys

$$x(\mathfrak{q}z) = x(z) + m. \tag{4.8}$$

The real part of this function is depicted in figure (Fig. 2) as a function of $\log z$. Define the fundamental cylinder to be the annulus $|\mathfrak{q}|^{1/2} < |z| < |\mathfrak{q}|^{-1/2}$. On the fundamental cylinder, the inverse function $z(x)$ is well defined. To first order in $\mathfrak{q}$, it looks like

$$z(x) = \frac{1}{1+m/x} + O(\mathfrak{q}). \tag{4.9}$$

Hence, we see that

$$z(x=\infty) = 1. \tag{4.10}$$

Now, let us have a look at the RHS of Eq. (4.5). We see that the set of its zeros is a curve whose branches are labeled by integers

$$z_n(x) = \mathfrak{q}^n \frac{Y(x-nm)}{Y(x+(1-n)m)}, \qquad n \in \mathbb{Z}, \tag{4.11}$$

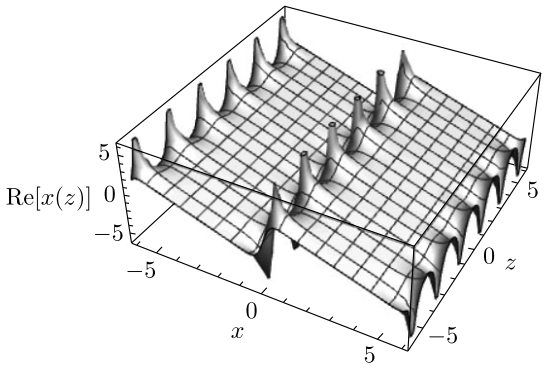

Fig. 2. $\mathrm{Re}[x(z)]$

each behaving like

$$z_n(x) \to \mathfrak{q}^n \quad \text{as} \quad x \to \infty. \tag{4.12}$$

In (4.9), we choose the $n = 0$ branch

$$z(x) = z_0(x) = \frac{Y(x)}{Y(x+m)}. \tag{4.13}$$

Thus, we obtain the identity

$$\frac{d}{dx} \log z(x) = \frac{1}{2} \int_{\mathbb{R}} \frac{f''(y)}{x-y}\, dy - \frac{1}{2} \int_{\mathbb{R}} \frac{f''(y)}{x-y+m}\, dy \tag{4.14}$$

for the limit profile function $f \in C^1(\mathbb{R})$, which is related to $Y(x)$ as in (2.18). From this we derive

$$\frac{d}{dx} \log z(x) = \frac{1}{z\, dx/dz} = \frac{1}{mF_{\mathfrak{q}}(z)}, \tag{4.15}$$

where

$$F_{\mathfrak{q}}(z) = \sum_{n \in \mathbb{Z}} \frac{z\mathfrak{q}^n}{(1 - z\mathfrak{q}^n)^2}. \tag{4.16}$$

One gets

$$\frac{1}{F_{\mathfrak{q}}(z(x))} = \frac{m}{2} \int_{\mathbb{R}} \frac{f''(y)}{x-y}\, dy - \frac{m}{2} \int_{\mathbb{R}} \frac{f''(y)}{x-y+m}\, dy. \tag{4.17}$$

The RHS of Eq. (4.17) has, as a function of x, two branch cuts a distance m apart from each other, with the opposite sign jumping across each. As $x \to \infty$, the RHS of (4.17) goes to zero as $(m/x)^2$, since

$$\int_{\mathbb{R}} f''(y)\, dy = 2, \tag{4.18}$$

in agreement with the LHS.

The quasiperiodicity of $x(z)$ implies that the branch cuts on the RHS correspond to the top and bottom edges of the fundamental cylinder in the z variable: $|z| = |\mathfrak{q}|^{1/2}$ and $|z| = |\mathfrak{q}|^{-1/2}$. Let us describe their locations explicitly.

For the bottom edge (parameterized by angle θ) one has

$$x(\mathfrak{q}^{1/2}e^{\mathrm{i}\theta}) = \mathrm{i}m\sin\theta g_{\mathfrak{q}}(\cos\theta), \tag{4.19}$$

where

$$g_{\mathfrak{q}}(\cos\theta) = 2\sum_{r\in\mathbb{Z}_{\geqslant 0}+1/2}\frac{\mathfrak{q}^r}{1-2\mathfrak{q}^r\cos\theta+\mathfrak{q}^{2r}}, \tag{4.20}$$

and for the upper edge we have

$$x(\mathfrak{q}^{-1/2}e^{\mathrm{i}\theta}) = x(\mathfrak{q}^{1/2}e^{\mathrm{i}\theta}) - m. \tag{4.21}$$

As $X(\theta) := -\mathrm{i}x(\mathfrak{q}^{1/2}e^{i\theta})/m$ is real for $\theta \in [-\pi,\pi]$ (it is depicted approximately for $\mathfrak{q} = 1/3$ in Fig. 3), we see that one branch cut is located on the real axis, and another one is shifted in the imaginary direction by $-m$. Since $X(\theta)$ is odd,

$$X(-\theta) = -X(\theta). \tag{4.22}$$

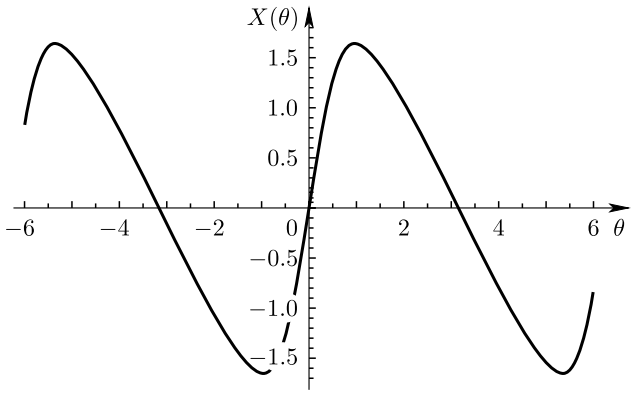

Fig. 3. $X(\theta)$.

It vanishes at $\theta = 0$ and $\theta = \pi$; therefore, it has a maximum $\theta_* \in (0,\pi)$:

$$X'(\theta_*) = 0. \tag{4.23}$$

From Eq. (4.27) below, it follows that it is unique. Accordingly, $\pm x_*$, with

$$x_* := \mathrm{i}mX(\theta_*), \tag{4.24}$$

are the ends of the branch cut located on the real axis in the x-plane (see Fig. 4).

This means that for any value $x \in (-x_*, x_*)$, there are two corresponding values $\theta_\pm(x)$:

$$x = \mathrm{i}mX(\theta_+(x)) = \mathrm{i}mX(\theta_-(x)). \tag{4.25}$$

We denote the upper side of the cut by C_+. It is parametrized by θ, running from $-\theta_*$ to θ_*. We denote the lower side of the cut by C_-. It is parametrized by θ, running from $-\pi$ to$-\theta_*$, then from θ_* to π (see Fig. 5). Therefore, the jump which we are after is equal to

$$\mathrm{i}\pi m f''(x) = \frac{1}{F_{\mathfrak{q}}(\mathfrak{q}^{1/2}e^{\mathrm{i}\theta_+})} - \frac{1}{F_{\mathfrak{q}}(\mathfrak{q}^{1/2}e^{\mathrm{i}\theta_-})}. \tag{4.26}$$

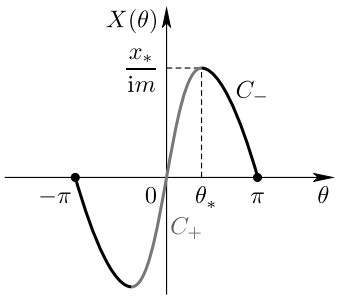

Fig. 4. $X(\theta)$ with colored sides of the cut.

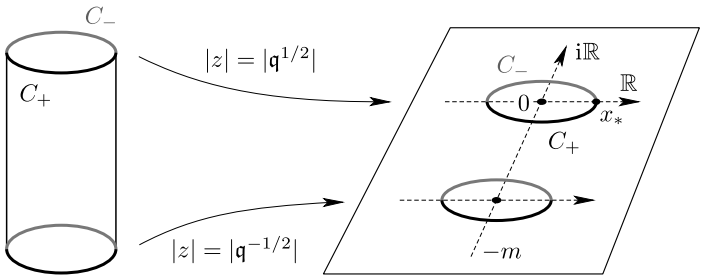

Fig. 5. Domain and image of $x(z)$.

As

$$X'(\theta) = F_{\mathfrak{q}}(\mathfrak{q}^{1/2}e^{i\theta}) = -\frac{\wp(\tau/2 + \theta/(2\pi))}{4\pi^2}, \tag{4.27}$$

the critical point θ_* is related to a zero of the Weierstrass function. The latter has two zeroes on the elliptic curve, one giving the maximum of $X(\theta)$ for real θ, and the other the minimum. Eq. (4.26) can be integrated once to give

$$f'(x) = \frac{\theta_+(x) - \theta_-(x)}{\pi} + 1, \tag{4.28}$$

giving an elliptic version of the arcsin law [6] of Vershik–Kerov. As the functions $\theta_+(x)$ and $\theta_-(x)$, defined so that they are continuous on the interval $(-x_*, x_*)$ with $\theta_+(x_*) = \theta_-(x_*)$, satisfy $\theta_-(-x_*) - \theta_+(-x_*) = 2\pi$, the choice of integration constant ensures that $f'(x_*) = -f'(-x_*) = 1$ (cf. Fig. 5).

5. Limits and Asymptotics

5.1. Edge Asymptotics. The functions $\theta_\pm(x)$ are transcendental, but the edge behavior of $f''(x)$ is easy to analyze: as $x \to \pm x_*$, $\theta \to \theta_*$, we can expand

$$X(\theta) = X(\theta_*) + \frac{1}{2}X''(\theta_*)(\theta - \theta_*)^2 + O\big((\theta - \theta_*)^3\big), \tag{5.1}$$

giving

$$\theta_\pm = \theta_* \pm \sqrt{\frac{2(x - x_*)}{\mathrm{i}mX''(\theta_*)}}, \tag{5.2}$$

which by simple calculations leads to

$$f''(x) \sim \frac{2}{\pi\sqrt{2\mathrm{i}mX''(\theta_*)(x - x_*)}} = \frac{\gamma}{\sqrt{x_* - x}}, \tag{5.3}$$

with

$$\gamma = 2^{5/4}3^{3/4}\pi^{-3/2}\left(1 - 504\sum_{n=1}^{\infty} n^5 \frac{\mathfrak{q}^n}{1-\mathfrak{q}^n}\right)^{-1/4}. \tag{5.4}$$

We can compare (5.3) to (2.24):

$$f''_{\mathrm{VK}}(x) \sim \frac{1}{\pi\sqrt{\Lambda}}\frac{1}{\sqrt{2\Lambda - x}}. \tag{5.5}$$

Even though the functional forms of the edge asymptotics of the limit shapes in the elliptic and in the Vershik–Kerov case are similar, a detailed comparison requires a more precise matching of the parameters. We do this by taking the confluent (Inozemtsev) limit

$$\begin{gathered} m \to \infty, \qquad \mathfrak{q} \to 0, \qquad z \to 0, \\ \mathfrak{q}^{1/2}m = -\mathrm{i}\Lambda\text{- fixed}, \qquad mz = y\text{- fixed}. \end{gathered} \tag{5.6}$$

In this limit, the measure in (3.1) reduces to (2.2). Next, the only terms left in the product from the RHS of (4.5) are

$$\left(1 - \frac{y}{Y(x)}\right)Y(x)\left(1 - y^{-1}\frac{\Lambda^2}{Y(x)}\right), \tag{5.7}$$

which is equal to

$$\chi(x) - \left(y + \frac{\Lambda^2}{y}\right), \tag{5.8}$$

and is in agreement with the limit of (4.4). From (4.19) and (4.4), one sees that

$$x(\mathfrak{q}^{1/2}e^{\mathrm{i}\theta}) \to 2\Lambda\sin\theta. \tag{5.9}$$

Hence, one has

$$\theta_+(x) = \vartheta_+^{\mathrm{VK}}\left(\frac{x}{2\Lambda}\right) := \arcsin\frac{x}{2\Lambda}, \qquad \theta_+(x) = \vartheta_-^{\mathrm{VK}}\left(\frac{x}{2\Lambda}\right) := \pi - \arcsin\frac{x}{2\Lambda}, \tag{5.10}$$

establishing the agreement between Eqs. (4.28) and (2.26).

5.2. Matching the Edge Behaviour. The Inozemtsev limit of (5.3),

$$f''(x) \sim \frac{2}{\pi\sqrt{2\mathrm{i}mX''(\theta_*)(x - x_*)}} \to \frac{1}{\pi\sqrt{\Lambda(2\Lambda - x)}}, \tag{5.11}$$

matches the edge behaviour of $f''_{\mathrm{VK}}(x)$,

$$f''_{\mathrm{VK}}(x) = \frac{1}{\pi\Lambda}\frac{1}{\sqrt{1 - (x/(2\Lambda))^2}} \sim \frac{1}{\pi\sqrt{\Lambda(2\Lambda - x)}}. \tag{5.12}$$

5.3. Expanding around the Vershik–Kerov Limit Shape. The comparison of the limit shape of our problem to that of (2.2) is an instructive exercise in perturbative renormalization. Naively, fixing $\Lambda = \mathrm{i}m\mathfrak{q}^{1/2}$ and varying $\mathfrak{q}$ for small $\mathfrak{q}$, we can find θ_*, $\theta_\pm(x)$ by expanding in $\mathfrak{q}^{1/2}$ (cf. (5.10)):

$$\begin{gathered} \theta_* = \frac{\pi}{2} - \mathfrak{q}^{1/2}\left(2 - \frac{8}{3}\mathfrak{q} + \frac{72}{5}\mathfrak{q}^2 - \frac{632}{7}\mathfrak{q}^3 + \frac{5462}{9}\mathfrak{q}^4 - \frac{47016}{11}\mathfrak{q}^5 + \cdots\right), \\ x_* = 2\Lambda(1 + 2\mathfrak{q} + 8\mathfrak{q}^3 - 29\mathfrak{q}^4 + 162\mathfrak{q}^5 + \cdots), \end{gathered} \tag{5.13}$$

which then leads to the singular expansion for $\theta_\pm(x)$ and $f(x)$,

$$\begin{aligned}\theta_\pm(x) &\stackrel{?}{=} \vartheta_\pm^{\mathrm{VK}}(\xi) - 2\mathfrak{q}^{1/2}\xi \mp 2\mathfrak{q}\frac{\xi^3}{\sqrt{1-\xi^2}} + 4\mathfrak{q}^{3/2}\xi\left(1+\frac{2}{3}\xi^2\right) + O(\mathfrak{q}^2),\\ f'(x) &\stackrel{?}{=} \frac{2}{\pi}\arcsin\xi - \frac{4\mathfrak{q}}{\pi}\frac{\xi^3}{\sqrt{1-\xi^2}} + O(\mathfrak{q}^2),\end{aligned} \tag{5.14}$$

with $\xi = x/(2\Lambda)$. There are, of course, no singular terms in $f'(x)$ as it is a monotone continuous function on $[-x_*, x_*]$ changing from -1 to $+1$. The solution to the puzzle is that the singularities reflect the $\mathfrak{q}$-dependence of the cut. If, instead of Λ, one keeps x_* fixed, the corresponding expansion becomes perfectly non-singular:

$$\begin{aligned}\theta_\pm(x) = \vartheta_\pm^{\mathrm{VK}}(y) &- 2\mathfrak{q}^{1/2}y\left(1 - \frac{4\mathfrak{q}}{3}y^2 + 4\mathfrak{q}^2\left(1-2y^2-\frac{4}{5}y^4\right)\right.\\ &- 20\mathfrak{q}^3\left(1+\frac{2}{5}y^2-\frac{16}{5}y^4-\frac{16}{35}y^6\right)\\ &\left.+ 61\mathfrak{q}^4\left(1+\frac{272}{61}y^2-\frac{224}{61}y^4-\frac{384}{61}y^6-\frac{256}{549}y^8\right)+\cdots\right)\\ &\mp 2\mathfrak{q}y\sqrt{1-y^2}\left(1-3\mathfrak{q}\left(1+\frac{2}{3}y^2\right)+6\mathfrak{q}^2\left(1+\frac{40}{9}y^2+\frac{8}{9}y^4\right)\right.\\ &\left.- 3\mathfrak{q}^3\left(1+38y^2+56y^4+\frac{16}{3}y^6\right)+\frac{7296}{5}\mathfrak{q}^4y^4\left(1+\frac{12}{19}y^2+\frac{2}{57}y^4\right)+\cdots\right),\end{aligned} \tag{5.15}$$

where $y = x/x_*$. For the values $\mathfrak{q} = 0, 0.01, 0.02, 0.05, 0.1, 0.2$ and $x_* = 1$, $f(x)$ is shown in (Fig. 6).

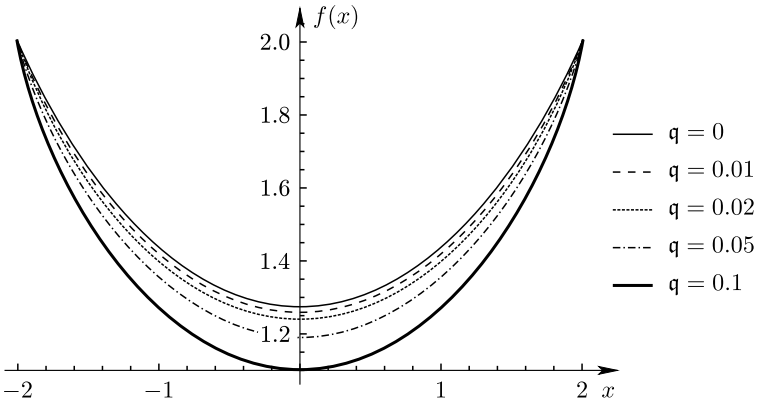

Fig. 6. $f(x)$ to the first few orders in $\mathfrak{q}$.

6. Conclusions and Future Directions

In this paper, we explored a one-parametric deformation $\boldsymbol{\mu}_{m,\mathfrak{q},\hbar}$ of the Plancherel measure on the set of Young diagrams and found its limit shape. Specifically, we kept the size fugacity $\mathfrak{q}$ finite and refined the parameter $m/\hbar \to \infty$.

There is a natural generalization of such a limit shape problem (motivated, e.g., by topological string theory and gauge theory [15], [9]) where the measure $\mu[\lambda]$ includes the chemical potentials for the generalized Casimirs $\mathbf{p}_k$. We introduce the sequence (t_k), $k = 1, 2, \ldots$, of formal variables, further introduce the formal function

$$\mathbf{t}(x) = \sum_{k=1}^{\infty} t_k x^k, \tag{6.1}$$

and define the measures (cf. [9])

$$\mu_{\Lambda,\hbar;\mathbf{t}}[\lambda] = \mu_{\Lambda,\hbar}[\lambda] e^{\mathbf{t}(\hbar c_\square)}, \qquad \mu_{m,\mathfrak{q},\hbar;\mathbf{t}}[\lambda] = \mu_{m,\mathfrak{q},\hbar}[\lambda] e^{\mathbf{t}(\hbar c_\square)}. \tag{6.2}$$

The limit shape is now governed by the analytic multi-valued function $Y(x)$, which behaves as $x + o(x^{-1})$ on the physical sheet such that, in the first case,

$$Y(x) + \Lambda^2 \frac{e^{\mathbf{t}(x)}}{Y(x)} \tag{6.3}$$

is an entire function of x. One cannot claim that (6.3) is a linear function of x as the LHS has an essential singularity at $x \to \infty$. However, the formal nature of variables t_k suggest that the Riemann surface of Y is still a two-sheeted cover of the x-plane. Also, the probabilistic nature of the problem shows that Y has a single cut on the physical sheet. By comparing the two terms in the LHS of (6.3), one concludes that Y is an analytic function on the curve $\mathcal{C}$

$$y + \frac{\widetilde{\Lambda}^2}{y} = x + \widetilde{v}, \tag{6.4}$$

where the parameters $(\widetilde{v}, \widetilde{\Lambda})$ are the formal functions of t_k such that at $t_k = 0$ they approach $(0, \Lambda)$. There are two special points $P_\pm$ where $x = \infty$. At P_+, $y \sim x$, and at P_-, $y \sim \Lambda^2 x^{-1} \to 0$. In other words, $(x, y) = (\infty, \infty)$ at P_+, and $(x, y) = (\infty, 0)$ at P_-. The function Y is found from the following conditions: it is holomorphic on $\mathcal{C}$ outside $P_\pm$, and it has the asymptotics

$$\begin{aligned} Y &\sim x, \qquad (x, y) \to P_+, \\ Y &\sim \Lambda^2 x^{-1} e^{\mathbf{t}(x)}, \qquad (x, y) \to P_-. \end{aligned} \tag{6.5}$$

Here is how one finds such a function. Define the functions $\Omega_k^\pm$ to be meromorphic functions on $\mathcal{C}$, holomorphic outside $P_\pm$, respectively, such that

$$\Omega_k^\pm = x^k + o(x^{-1}), \qquad (x, y) \to P_\pm. \tag{6.6}$$

It follows that

$$x^k = \Omega_k^+(y) + \Omega_k^-(y) - \omega_k, \tag{6.7}$$

where

$$\omega_k = \Omega_k^+(P_-) = \Omega_k^-(P_+) = \frac{1}{2\pi \mathrm{i}} \oint_{|y| = |\widetilde{\Lambda}|} \frac{dy}{y} x^k. \tag{6.8}$$

Then

$$Y = y \exp\left\{ \sum_k t_k (\Omega_k^-(y) - \omega_k) \right\} \tag{6.9}$$

has the correct asymptotics at both $P_\pm$ and continues analytically across the cuts of the y-function, provided that the matching equations at the branch-points

$$\widetilde{\Lambda}^2 \exp\left\{ - \sum_k t_k \omega_k \right\} = \Lambda^2 \tag{6.10}$$

hold, and that the vanishing period

$$0 = - \oint x \frac{dY}{Y} = \widetilde{v} + \sum_k t_k \operatorname{Coeff}_{y^{-1}} \Omega_k^- \tag{6.11}$$

guarantees the correct asymptotics $Y \sim x + o(x^{-1})$ on the physical sheet. This gives two equations for the two unknowns $(\widetilde{v}, \widetilde{\Lambda})$. For example, setting $t_2 = t_3 = \cdots = 0$, one easily recovers the Lambert solution found in [10]:

$$\widetilde{v} = -t_1 \widetilde{\Lambda}^2, \qquad \Lambda^2 = \widetilde{\Lambda}^2 e^{-2t_1 \widetilde{\Lambda}^2}, \tag{6.12}$$

with its finite convergence radius typical of Whitham hierarchies [7]. The second case of (6.2) and other generalizations will be presented in the companion paper [5].

There is yet another class of limit shape problems where the parameter $m/\hbar$ in $\boldsymbol{\mu}_{m,\mathfrak{q},\hbar}$ is fixed while the instanton fugacity $\mathfrak{q}$ approaches 1– a Hardy-Ramanujan limit. In the special case where $m = 0$, the limit shape curve is the celebrated

$$e^{-a} + e^{-b} = 1, \qquad a, b \geqslant 0. \tag{6.13}$$

Generalizations to $m \neq 0$ will be considered elsewhere.

Finally, all the measures discussed above were symmetric under $\lambda \mapsto \lambda^t$. Four-dimensional gauge theory [12] suggests yet another natural generalization in which the weight of the box $\square \in \lambda$ depends separately on the arm $a_\square = \lambda_i - j$ and the leg $l_\square = \lambda^t_j - i$. For example,

$$\boldsymbol{\mu}_{m,\mathfrak{q};\varepsilon_1,\varepsilon_2}[\lambda] = \frac{1}{Z_{2^*}(m,\mathfrak{q};\varepsilon_1,\varepsilon_2)} \mathfrak{q}^{|\lambda|} \times \prod_{\square} \left(1 + \frac{m}{\varepsilon_1(a_\square + 1) - \varepsilon_2 l_\square}\right)\left(1 + \frac{m}{-\varepsilon_1 a_\square + \varepsilon_2(l_\square + 1)}\right). \tag{6.14}$$

Of course, such measures are well known to mathematicians under the name of discrete β-ensembles, Jack processes, etc. [1], [2]. We know [13] that the partition function exponentiates

$$Z_{2^*}(m,\mathfrak{q};\varepsilon_1,\varepsilon_2) \sim \exp\left\{\frac{1}{\varepsilon_2}\right\} W(m,\mathfrak{q};\varepsilon_1), \tag{6.15}$$

when $\varepsilon_2 \to 0$ with $m, \varepsilon_1, \mathfrak{q}$ kept constant. The corresponding limit shape is described by a quantum spectral curve [4].

7. Appendix. Proof of the Factorization Formula

The $\hbar \to 0$ limit of the normalized qq-character, including the higher times, is given by

$$\chi(x) = \phi(\mathfrak{q}) \sum_\lambda \mathfrak{q}^{|\lambda|} \prod_{\square \in \lambda} e^{\mathbf{t}(x + mc_\square)} \frac{\prod_{\square \in \partial_+ \lambda} Y(x + mc_\square)}{\prod_{\square \in \partial_- \lambda} Y(x + mc_\square)}. \tag{7.1}$$

Motivated by [4], we prove the following.

Lemma. *Let z be an indeterminate. The following identity holds.*

$$\begin{aligned} Y(x) \cdot \prod_{n=0}^{\infty} \left(1 - z\mathfrak{q}^n e^{\widehat{t}(x+mn)} \frac{Y(x + (n+1)m)}{Y(x+nm)}\right) \\ \times \prod_{n=1}^{\infty} \left(1 - z^{-1}\mathfrak{q}^n e^{-\widehat{t}(x-mn)} \frac{Y(x-nm)}{Y(x-(n-1)m)}\right) \\ = \sum_{n=1}^{\infty} (-z)^n \mathfrak{q}^{(n^2-n)/2} \exp\left\{\sum_{j=0}^{n-1} \widehat{t}(x+jm)\right\} \chi(x+nm) + \chi(x) \\ + \sum_{n=1}^{\infty} (-z)^{-n} \mathfrak{q}^{(n^2+n)/2} \exp\left\{-\sum_{j=1}^{n} \widehat{t}(x-jm)\right\} \chi(x-nm), \end{aligned} \tag{7.2}$$

where $\widehat{t}(x)$ is the unique formal power series in x such that $\widehat{t}(0) = 0$, and solving

$$t(x) = \widehat{\mathbf{t}}(x) - \widehat{\mathbf{t}}(x - m). \tag{7.3}$$

Proof. By a simple cancellation of factors, the formula for the qq-character can be rewritten as

$$\chi(x) = \sum_{\lambda} \mathfrak{q}^{|\lambda|} \prod_{\square \in \lambda} e^{t(x+mc_\square)} \prod_{j=1}^{\lambda_1} \frac{Y(x + m(\lambda_j^t - j + 1))}{Y(x + m(\lambda_j^t - j))} Y(x - m\lambda_1). \tag{7.4}$$

Expanding the brackets on the LHS of formula (7.2), one obtains

$$\sum_{r,s \geqslant 0} \sum_{\substack{n_0 > n_1 > \cdots > n_{r-1} \geqslant 1 \\ 0 \leqslant k_0 < k_1 < \cdots < k_{s-1}}} (-z)^{r-s} \prod_{i=0}^{r-1} \mathfrak{q}^{n_i - 1} e^{\widehat{t}(x + (n_i - 1)m)} \prod_{i=0}^{s-1} \mathfrak{q}^{k_i + 1} e^{-\widehat{t}(x - (k_i + 1)m)}$$
$$\times \prod_{i=0}^{r-1} \frac{Y(x + n_i m)}{Y(x + (n_i - 1)m)} \cdot Y(x) \cdot \prod_{i=0}^{s-1} \frac{Y(x - (k_i + 1)m}{Y(x - k_i m)}. \tag{7.5}$$

Note that the two sets of strictly increasing numbers $n_0 > n_1 > \cdots > n_{r-1} \geqslant 1$ and $0 \leqslant k_0 < k_1 < \cdots < k_{s-1}$ encode information about the Young diagram λ and an additional integer, which could be interpreted as a shift of the Young diagram perpendicular to the main diagonal. The dictionary is the following. The shift is equal to $p = r - s$. The positive integers n_j define the lengths of the first r-columns, and k_i define the length of the first s-rows through the formulas

$$n_j = \lambda_{j+1}^t - j + p, \qquad j = 0, \ldots, r - 1, \tag{7.6}$$
$$k_{s-i} = \lambda_i - i - p, \qquad i = 1, \ldots, s. \tag{7.7}$$

This data uniquely determines the diagram. Notice that, given λ and p, the numbers r and s are uniquely determined as such values of i and j where the expressions $\lambda_i - i - p$, $\lambda_{j+1}^t - j + p$ change sign. With this substitution, the above expression can be rewritten as

$$\sum_{p \in \mathbb{Z}} \sum_{\lambda} (-z)^p \prod_{j=0}^{r-1} \mathfrak{q}^{\lambda_{j+1}^t - j + p - 1} e^{\widehat{t}(x + m(\lambda_{j+1}^t - j + p - 1))} \prod_{i=1}^{s} \mathfrak{q}^{\lambda_i - i - p + 1} e^{\widehat{t}(x + m(\lambda_i - i - p + 1))} \cdot Y(x)$$
$$\times \prod_{j=0}^{r-1} \frac{Y(x + (\lambda_{j+1}^t - j + p)m)}{Y(x + (\lambda_{j+1}^t - j + p - 1)m)} \cdot \prod_{i=1}^{s} \frac{Y(x - (\lambda_i - i - p + 1)m)}{Y(x - (\lambda_i - i - p)m)}. \tag{7.8}$$

Now we need to match every multiple in the product to every multiple in the expression (7.4), shifted by p. Let us denote

$$\begin{aligned} \mathrm{LHS}(\lambda, p) &= \prod_{j=0}^{r-1} \frac{Y(x + (\lambda_{j+1}^t - j + p)m)}{Y(x + (\lambda_{j+1}^t - j + p - 1)m)} \cdot Y(x) \cdot \prod_{i=1}^{s} \frac{Y(x - (\lambda_i - i - p + 1)m)}{Y(x - (\lambda_i - i - p)m)}, \\ \mathrm{RHS}(\lambda, p) &= Y(x - m(\lambda_1 - p)) \prod_{j=1}^{\lambda_1} \frac{Y(x + m(\lambda_j^t - j + 1 + p)}{Y(x + m(\lambda_j^t - j + p))}. \end{aligned} \tag{7.9}$$

We are going to prove that $\mathrm{LHS}(\lambda, p) = \mathrm{RHS}(\lambda, p)$ by induction on the number of boxes in the Young diagram.

The base of the induction is the case when $\lambda = \varnothing$, and either $r = 0$, and hence $s = -p$, or $s = 0$, and $r = p$.

Let us consider the case $r = 0$ first. The $\mathrm{LHS}(\varnothing, -s)$ of the formula above then takes the form

$$Y(x) \cdot \prod_{i=1}^{s} \frac{Y(x + (i + p - 1)m)}{Y(x + (i + p)m)}, \tag{7.10}$$

which, after cancelling all factors, is equal to the $\mathrm{RHS}(\varnothing, -s) = Y(x + mp)$. Now letting $s = 0$, one has

$$\mathrm{LHS}(\varnothing, r) = \prod_{j=0}^{r-1} \frac{Y(x + (r - j)m)}{Y(x + (r - j - 1)m)} Y(x - (r - 1)) = Y(x + rm), \tag{7.11}$$

which is equal to the RHS $(\varnothing, r)$.

For the induction step, let us assume that we are adding one box to the kth row. For the LHS, the cases $k - \lambda_k - 1 + p \geqslant 0$ and $k - \lambda_k - 1 + p < 0$ should be treated separately because they affect the product of the first r factors or the last s factors correspondingly, but eventually the final result is the same:

$$\frac{\mathrm{LHS}(\lambda + 1_k, p)}{\mathrm{LHS}(\lambda, p)} = \frac{Y(x - (\lambda_k - k - p + 2)m)}{Y(x - (\lambda_k - k - p + 1)m)} \frac{Y(x - (\lambda_k - k - p)m)}{Y(x - (\lambda_k - k - p + 1)m)}. \tag{7.12}$$

By analogous calculation, the same is true for the RHS. Hence the formula is proven.

Now let us deal with the factors depending on $\widehat{t}(x)$. On the LHS, we have the function in the exponent

$$d(\lambda, p) := \sum_{i=0}^{r-1} \widehat{t}(x + m(n_i - 1)) - \sum_{j=0}^{s-1} \widehat{t}(x - m(k_j + 1)). \tag{7.13}$$

Similarly to the discussion above, we can calculate the change under the addition of a box into the kth row:

$$d(\lambda + 1_k, p) - d(\lambda, p) = \widehat{t}(x - m(\lambda_k - k - p + 1)) - \widehat{t}(x - m(\lambda_k - k - p + 2)). \tag{7.14}$$

For the RHS, we would like to look at the function

$$d'(\lambda, p) := \sum_{\square \in \lambda} t(x + m(p + c_\square)) = \sum_{\square \in \lambda} \widehat{t}(x + m(p + c_\square)) - \widehat{t}(x + m(p - 1 + c_\square)). \tag{7.15}$$

Hence,

$$d'(\lambda + 1_k, p) - d'(\lambda, p) = \widehat{t}(x - m(\lambda_k - k - p + 1)) - \widehat{t}(x - m(\lambda_k - k - p + 2)). \tag{7.16}$$

So the induction step is proven. And for the base we have

$$d'(\varnothing, p) = 0. \tag{7.17}$$

However,

$$d(\varnothing, p) = \begin{cases} \displaystyle\sum_{j=0}^{p-1} \widehat{t}(x + jm), & p \geqslant 0, \\ \displaystyle -\sum_{j=1}^{-p} \widehat{t}(x - jm), & p < 0, \end{cases} \tag{7.18}$$

which are exactly the factors we see in (7.2). The last step is to compare the $\mathfrak{q}$ dependence. This proof is carried out by the same trick.

Note that the proof is similar to the fermionic proof of the Jacobi triple product identity. $\square$

Acknowledgements

We have greatly benefited from the patient explanations of I. Krichever and A. Okounkov.

Funding

Research is partly supported by NSF PHY Award 2310279.

Conflict of Interest

The authors of this work declare that they have no conflicts of interest.

References

[1] A. Borodin, G. Olshanski, "Z-measures on partitions and their scaling limits", *European J. Combin.*, **26**:6 (2005), 795–834.
[2] E. Dimitrov, A. Knizel, "Asymptotics of discrete β-corners processes via two-level discrete loop equations", *Probab. Math. Phys.*, **3**:2 (2022), 247–342.
[3] R. Donagi, E. Witten, "Supersymmetric Yang–Mills theory and integrable systems", *Nuclear Phys. B*, **460**:2 (1996), 299–334.
[4] A. Grekov, N. Nekrasov, *Elliptic Calogero–Moser system*, *crossed and folded instantons*, *and bilinear identities*, arXiv: 2310.04571.
[5] A. Grekov, N. Nekrasov, "Vershik–Kerov in higher times and higher spaces" (to appear).
[6] A. M. Vershik, S. V. Kerov, "Asymptotics of the Plancherel measure of the symmetric group and the limiting form of Young tableaux", *Soviet Math. Dokl.*, **18** (1977), 527–531.
[7] I. M. Krichever, "The τ-function of the universal Whitham hierarchy, matrix models and topological field theories", *Comm. Pure Appl. Math.*, **47**:4 (1994), 437–475.
[8] B. F. Logan, L. A. Shepp, "A variational problem for random Young tableaux", *Adv. Math.*, **26**:2 (1977), 206–222.
[9] A. S. Losev, A. Marshakov, N. A. Nekrasov, *Small instantons*, *little strings and free fermions*, arXiv: hep-th/0302191.
[10] A. Marshakov, N. A. Nekrasov, "Extended Seiberg–Witten theory and integrable hierarchy", *J. High Energy Phys.*, **2007**:1 (2007), 104, 39 pp.
[11] N. A. Nekrasov, A. Okounkov, "Seiberg–Witten theory and random partitions", in: *The unity of mathematics. In honor of the ninetieth birthday of I. M. Gelfand*, Progr. Math., vol. 244, Birkhäuser Boston, Inc., Boston, MA, 2006, pp. 525–596.
[12] N. A. Nekrasov, "Seiberg–Witten prepotential from instanton counting", *Adv. Theor. Math. Phys.*, **7**:5 (2003), 831–864.
[13] N. Nekrasov, "BPS/CFT correspondence: non-perturbative Dyson–Schwinger equations and qq-characters", *J. High Energy Phys.*, **2016**:3 (2016), 181, 70 pp.
[14] N. Nekrasov, V. Pestun, *Seiberg–Witten geometry of four-dimensional $\mathcal{N} = 2$ quiver gauge theories*, arXiv: 1211.2240v2.

[15] A. Okounkov, R. Pandharipande, *Gromov–Witten theory*, *Hurwitz theory*, *and completed cycles*, arXiv: math/0204305.
[16] C. Vafa, E. Witten, "A strong coupling test of S-duality", *Nuclear Phys. B*, **431**:1-2 (1994), 3–77.

Andrei M. Grekov
Yang Institute for Theoretical Physics,
Stony Brook University, Stony Brook, USA
E-mail: andrei.grekov@stonybrook.edu

Nikita A. Nekrasov
Simons Center for Geometry and Physics,
Stony Brook University, Stony Brook, USA;
Yang Institute for Theoretical Physics,
Stony Brook University, Stony Brook, USA
E-mail: nnekrasov@scgp.stonybrook.edu

Received February 5, 2024
In final form March 11, 2024
Accepted March 18, 2024